



Article

Groundwater Management in an Uncommon and Artificial Aquifer Based on K_c Approach and MODIS ET Products for Irrigation Assessment in a Subtropical Island

Zhenglun Yang ¹, Changyuan Tang ^{1,*}, Hasi Bagan ², Shunichi Satake ³, Madoka Orimo ⁴, Koichiro Fukumoto ⁵ and Guangwei Wang ¹

- ¹ Graduate School of Horticulture, Chiba University, 648 Matsudo, Matsudo-City 271-8510, Chiba, Japan
² School of Environmental and Geographical Sciences, Shanghai Normal University, Shanghai 200234, China
³ Asahi Engineering Co., Ltd., 2-1 Shimomiyabicho, Shinjuku-ku, Tokyo 162-0822, Japan
⁴ Research and Development Center, Nippon Koei Co., Ltd., 2304, Inarihara, Tsukuba-shi 300-1259, Ibaraki, Japan
⁵ Nippon Koei Co., Ltd., 5-4 Kojimachi, Chiyoda-ku, Tokyo 102-8539, Japan
* Correspondence: cytang@faculty.chiba-u.jp; Tel.: +81-047-308-8911

Abstract: Groundwater is a critical resource in remote and isolated islands where rainfall hardly provides a continuous and even water supply. In this paper, in a very rare and uncommonly found artificial aquifer on Miyako Island, far away from the main continent of Japan, with limited experimental results of evaluations of crop water requirement, MODIS ET together with crop ET_c estimated from K_c coefficient from the nearest island were compared to determine the reliability of the MODIS ET and FAO-56-based ET_c value. The testified K_c approach for sugarcane ET was used to assess the risk of irrigation water shortages using historical metrological data and to predict the future risk of irrigation agriculture under different scenarios of GCM models. It was shown that FAO-56-based ET_c and MOD16A2 were both applicable for crop evapotranspiration on the island. Then, the response of groundwater storage to gross irrigation water requirement was analyzed to clarify the effect of irrigation on groundwater storage and the risk of groundwater depletion under current and future climatic conditions. Results showed that the construction of the dam efficiently secured the irrigation of sugarcane. Using historical climatic data (1951–2021), the influence of estimated irrigation water requirements on groundwater showed that in 296 out of 852 months, irrigation was heavily required. Over a 71 year period, there was absolutely no water for irrigation four times, or nearly once every 18 years. Under the future projected climate from four bias-corrected GCM models with two emission scenarios (2022–2100), the risk of groundwater depletion both in terms of frequency and duration will increase. Therefore, there is a need for either improvement of irrigation water management or additional construction of artificial aquifers on the island. The study proved the value of ET derived from remote sensing in areas lacking the support of experimental results. The methodology developed in the study can be potentially used to evaluate long-term irrigation demand and groundwater management over dry periods for engineering design or dam construction globally.

Keywords: artificial aquifer; irrigation water requirement; sugarcane; MOD16A2 model; SSEBop model; climate change



Citation: Yang, Z.; Tang, C.; Bagan, H.; Satake, S.; Orimo, M.; Fukumoto, K.; Wang, G. Groundwater Management in an Uncommon and Artificial Aquifer Based on K_c Approach and MODIS ET Products for Irrigation Assessment in a Subtropical Island. *Remote Sens.* **2022**, *14*, 6304. <https://doi.org/10.3390/rs14246304>

Academic Editors: Sayed M. Bateni and Tongren Xu

Received: 30 October 2022

Accepted: 1 December 2022

Published: 13 December 2022

Publisher's Note: MDPI stays neutral with regard to jurisdictional claims in published maps and institutional affiliations.



Copyright: © 2022 by the authors. Licensee MDPI, Basel, Switzerland. This article is an open access article distributed under the terms and conditions of the Creative Commons Attribution (CC BY) license (<https://creativecommons.org/licenses/by/4.0/>).

1. Introduction

Globally, there are 175,000 islands covering one-sixth of the Earth's total land surface with more than 600 million inhabitants, according to Global Island Partnership (GLISP, 2019 <http://www.glispa.org/about>, accessed on 23 January 2020). Most of these small islands often face a series of challenges regarding the supply of freshwater and food, climate change, and natural disasters [1]. Owing to their remote distance from the major continents for water supply and their short distances of rivers to catch enough precipitation, such islands

can hardly supply enough water continuously and uniformly for agriculture and people's livings [2–4]. To solve the recurring water shortage in these regions, several methods such as rainwater harvesting [5–7], fog harvesting [8,9], seawater desalination [10–12], and water diversion [13] are used. Groundwater is another valuable source of water supply. However, the short flow distance of the island aquifer to the surrounding seawater limits the capacity of groundwater storage. How to solve water shortages during the dry season driven by climate change [3] is a mounting challenge in the world [14].

Groundwater is critical and a ubiquitous concern for human life, providing an estimated 36, 42, and 27%, respectively, of global domestic, agricultural, and industrial water use [15]. Groundwater in small islands usually occurs as freshwater that floats on the underlying seawater [16,17]. For many island inhabitants, groundwater is often the only source of water supply [18], and substantial groundwater extraction for irrigation often results in seawater intrusion, for instance in the Pacific Small Island Developing States [19].

In past decades, considering the difficulties in harvesting surface water, subsurface dams are increasingly constructed in remote islands to stop groundwater flow so as to make it available for drinking and irrigation [20]. Like surface reservoirs, subsurface dams are a form of artificial underground aquifer suitable for storing water in pore spaces, rock fissures, or caves and can minimize water loss to the sea. The evaluation of water management in such artificial aquifer systems can provide valuable guidance for future construction of dams and better water management in such islands of the world.

Water management in such islands or similar areas lacking observational and experimental data is always the key focus of global hydrological studies, even though observations and experiments have been expended in recent decades [21,22]. Accurate estimation of key hydrological elements such as crop evapotranspiration (ET_c) and irrigation water requirements is of great significance to agricultural water management.

Determining the evapotranspiration of a crop is crucial in estimating the crop's irrigation requirements from weather variables [23–27]. There are many approaches for estimating ET. Aside from field experiments or direct observations and crop models, the FAO Penman–Monteith method (FAO-56) has been considered as a universal standard and most widely used approach for ET_c estimation in the last two decades [28]. In this method, as weather data for the calculation of ET_0 is easily available in most regions, crop coefficient (K_c) is the key index commonly required in determining irrigation water requirements of farmland. However, in many remote and underdeveloped areas, K_c is difficult to obtain through long-term field experiments. The K_c values from FAO-56 are based on the average values of the world and therefore are limited for use under local climatic conditions.

On the other hand, the development of ET estimation is becoming quickly available, both at global and regional scales [29,30]. Satellite-based diagnostic remote sensing ET such as MOD16A2 and SSEBop have comparable accuracy [31,32] and cover even the tiny and remote islands. They can also be used to estimate evapotranspiration and crop irrigation demands [31,33,34]. However, different approaches and ET products could lead to differences in estimating irrigation water requirements [35]. Moreover, the availability of high-resolution remote sensing ET data is always short in duration or limited to times after the launch of the MODIS satellite and therefore less applicable for long-term irrigation evaluation. Alternatively, as real estimated ET value is similar to ET_c , remote sensing ET data could potentially support the evaluation of crop coefficient from nearby or similar conditions. Furthermore, a joint evaluation of the local K_c value based on remote sensing ET data could potentially be used to determine the reliability of the K_c value in estimating irrigation water requirements for the long-term management of agricultural water resources.

In this study, an artificial aquifer named the Sunagawa Subsurface Dam, constructed in 1993 on Miyako Island, Japan [36], was chosen as the research case. It is a very rare artificial aquifer developed using the natural porous limestone by constructing an underground dam for irrigation water supply. After the construction of the dam, demand for agricultural irrigation increased, and thus there is an urgent concern about the risk of groundwater

depletion. The objectives of the study were to determine the reliability of the Kc coefficient using MODIS ET products for the evaluation of irrigation water demand, and then to assess the risk of groundwater shortage or the effectiveness of the artificial dam for securing an irrigation water supply under current and future climates.

2. Methods and Materials

2.1. Site Description

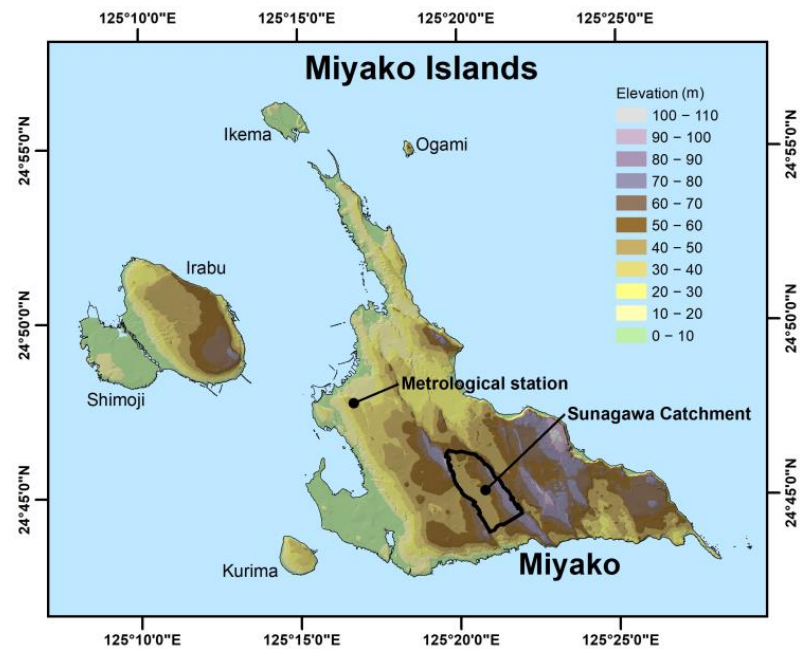
The study area is located on Miyako Island (24°47.6'N, 125°16.7'E) in Japan (Figure 1a). Miyako Island, as the largest island in the Miyako Islands (Figure 1a), is an isolated island belonging to the Ryukyu Archipelago and surrounded by the Pacific Ocean with a mean annual temperature of 23.4 °C. The mean annual precipitation of 2113.0 mm is greatly influenced by typhoons.

Sunagawa catchment is located in the southern part of the Miyako Island and covers an area of 7.2 km². The catchment is separated by two fault hills running from the northwest to the southeast direction in both sides of the valley. Owing to the high penetration of the limestone, there is no river in the catchment, and rainwater fully recharges into the aquifer and then, before the dam was constructed [37,38], would quickly flow out of the catchment into the ocean, causing water shortages in the non-typhoon season.

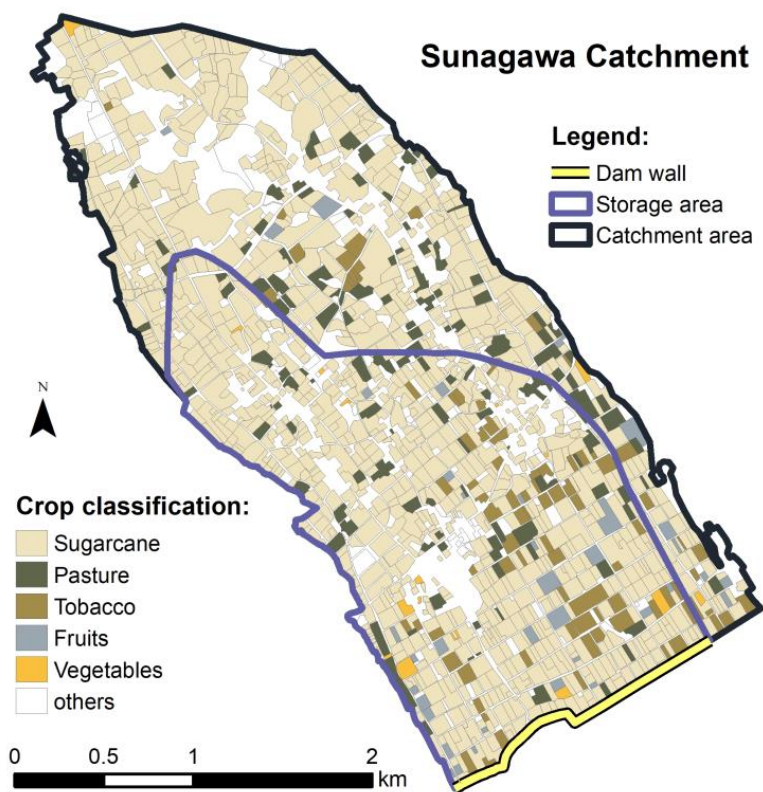
The most important reason for the construction of the Sunagawa subsurface dam was for irrigation water supply. The 1.7 km long artificial subsurface dam was built in 1993 downstream of the Sunagawa Catchment [39]. The dam extends as deep as 50 m, of which 31 m is above sea level [40] (Figure 1b). The porous limestone over the impermeable mudstone forms a good aquifer formation with an effective storage capacity of 6.8 million m³ and a total storage capacity of 9.5 million m³ [40,41]. The groundwater, which is a natural accumulation of rainwater underground, is pumped and transported through pipes to the tanks on the top of the hills for irrigation in the home and neighboring catchments. Due to the success of the subsurface dam on Miyako Island, the construction of more of such groundwater dams is being considered on such islands.

Even though annual precipitation in the subtropical island is high, it has a strong variation with extreme wet and dry periods. Like in most small islands, farmlands in the catchment are artificially reclaimed lands with dark-red soils (Shimajiri-mahji in Japanese classification) with thickness of 0.3–1 m and limited soil water-holding capacity [40,42]. During the land improvement project, the soil was first removed from the top of the limestone, the limestone was then leveled, and the stripped soil was finally covered back on top of the limestone. However, in fields reclaimed in this way, the thickness of the soil layer generally does not exceed 60 cm [43]. The growth of crops, especially sugarcane, often requires continuous replenishment of irrigation water. After the construction of the dam, demand for agricultural irrigation has been increasing, and thus there is an increasing concern about the shortage of groundwater supply, especially after experiencing recent warnings of groundwater depletion.

Figure 1b shows our land use classification map from a field survey for the catchment, of which 75.1% is farmland. Sugarcane, pasture, leaf tobacco, greenhouse fruits, and vegetables, respectively, account for 80.9, 9.2, 6.6, 2.5, and 0.8% of the farmland. As the main agricultural product, sugarcane is cultivated in three ways (summer planting, ratoon, and spring planting), accounting, respectively, for 60, 34, and 6% [38]. Summer cane is planted in August to September and harvested one and a half years later. Spring cane is planted in January to March and harvested the next January to March. Often, the root part of summer and spring cane is left after harvest for regrowth. Such ratoon cane is usually harvested once a year, and such a practice lasts for two growing years [41].



(a)



(b)

Figure 1. Maps of the study area: (a) topographical map of Miyako Island; (b) land use map for 2015 in Sunagawa catchment.

Sugarcane often requires continuous replenishment of irrigation during the dry season, which is largely done using sprinkler systems. Since there is a lack of an irrigation guidance and accounting system, irrigation water is often overused by local farmers to ensure that there is no soil water deficit.

2.2. Meteorological and Remote Sensing Dataset

Precipitation data for Miyako Island is available for 1951–2021 from the Japan Meteorological Agency at <http://www.data.jma.go.jp/obd/stats/etrn/index.php>, accessed on 25 October 2022. The collected meteorological data including daily temperature, rainfall, relative humidity, and sunshine hours were used to estimate evapotranspiration.

Two remote sensing ET products were collected, including the Moderate Resolution Imaging Spectroradiometer (MODIS) MOD16A2 model [44] for 2006–2019 and the Operational Simplified Surface Energy Balance (SSEBop) model [45] for 2006–2020. The ET from MOD16A2 is based on the Penman–Monteith equation by accounting for both surface energy partitioning and atmospheric drivers in 8-day and monthly timescale at 500 m spatial resolution (<https://lpdaac.usgs.gov/products/mod16a2v006/>, accessed on 1 December 2021). The SSEBop ET is monthly ET at 1 km spatial resolution and available at the USGS FEWS NET Data Portal (<https://earlywarning.usgs.gov/fews>, accessed on 1 December 2021).

2.3. Future Climate Change Data

A climate data set on future climate change on Miyako Island was downloaded from <https://www.nies.go.jp/doi/10.17595/20200415.001-e.html>, accessed on 1 March 2022 from the National Institute for Environmental Studies, Japan [46]. The data set is based on four GCMs (MIROC5, MRI-CGCM3, HadGEM2-ES, and GFDL-CM3) selected from CMIP5 and two GHGs emission pathways (RCP 2.6 and RCP 8.5). It is bias-corrected based on the downscaling method of CDFDM proposed by Iizumi et al. [47–50] using Japan's historical climate data. Daily data for seven variables such as daily mean, max, and min temperature, precipitation, solar radiation, wind speed, and relative humidity were averaged into monthly data for the period 1980–2100.

2.4. Flow Chart of the Methodology

The flow chart in Figure 2 illustrates the procedures to calculate irrigation water use from an aquifer or the amount of groundwater recharge. Firstly, three kinds of ET data (in mm), respectively, from the FAO-56 approach, MOD16A2 product, and SSEBop product were prepared. Then three kinds of ET data (in mm) were used to convert data into irrigation water demand (both in mm and m^3), when precipitation is not sufficient to supply water for crop ET ($ET-P > 0$), and groundwater recharge, when precipitation is more than enough to meet crop ET demand ($ET-P < 0$). During the conversion process, the area difference between the area of catchment and the irrigated crop area both in the home catchment and in the neighboring catchments is considered. Similarly, for groundwater, the water table is directly converted to groundwater storage (in mm) using the official H-Q formula to avoid the misunderstanding of combinational use of groundwater depth and groundwater storage in m^3 and in mm, respectively.

The detailed calculation processes are described hereafter.

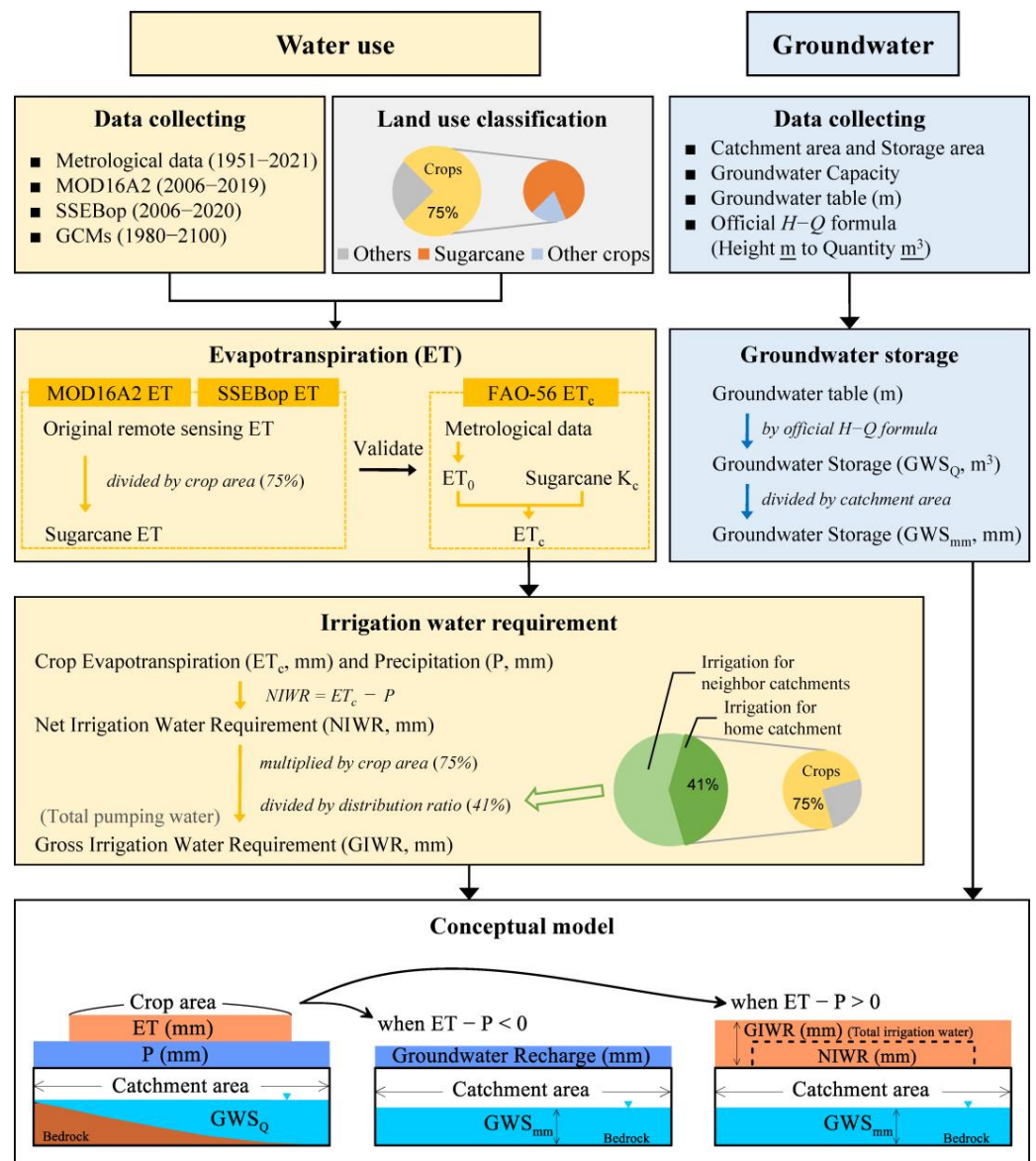


Figure 2. Flow chart of the methodology for the estimation of irrigation water requirement and influence on groundwater storage. The estimation of irrigation water requirement is based on a joint approach of FAO-56 for ET_c and MODIS ET.

2.5. FAO56-Based Sugarcane Evapotranspiration

Considering that the two MODIS-based ET products are not temporally long enough for evaluation of long-term water management, the most widely applied crop water requirement method by Allen et al. [28] was used for sugarcane, the dominant crop. The method is based on the crop coefficient (K_c) and reference evapotranspiration (ET_0) approaches.

According to Allen et al. [28], ET_0 is potential evapotranspiration and refers to evapotranspiration at a crop height of 0.12 m, a fixed surface resistance of 70 s m^{-1} , and an albedo of 0.23, driven by FAO56 (the Penman-Monteith method) (<http://www.fao.org/docrep/X0490E/x0490e06.htm>, accessed on 15 October 2021) [28].

$$ET_0 = \frac{0.408\Delta(R_n - G) + \gamma \frac{900}{T+273} u_2 (e_s - e_a)}{\Delta + \gamma(1 + 0.34u_2)} \quad (1)$$

where ET_0 is reference evapotranspiration (mm day^{-1}); R_n is net radiation at crop surface ($\text{MJ m}^{-2} \text{ day}^{-1}$); G is soil heat flux density ($\text{MJ m}^{-2} \text{ day}^{-1}$); T is mean daily air temperature

at 2 m height ($^{\circ}\text{C}$); u_2 is wind speed at 2 m height (m s^{-1}); e_s is saturation vapor pressure (kPa); e_a is actual vapor pressure (kPa); $e_s - e_a$ is vapor pressure deficit (kPa); Δ is slope vapor pressure curve ($\text{kPa } ^{\circ}\text{C}^{-1}$); and γ is psychrometric constant ($\text{kPa } ^{\circ}\text{C}^{-1}$).

For K_c , there are no directly measured water balance data for sugarcane in such a remote island. However, quite a few papers have investigated K_c of sugarcane in different regions of the world. These include the work done for the world average [28], American subtropical regions [51], Australia [52], and several sites in tropical regions [53–56]. Based on field experiments on lysimeter water balance in Naha, 300 km away from the Miyakojima island, Hossain et al. [57] estimated monthly K_c for summer cane and spring cane (see Figure 3). Since the percentage of spring cane is limited (only 6%) in the catchment, K_c for summer cane was used to calculate actual evapotranspiration as [28]

$$ET_c = K_c \times ET_0, \quad (2)$$

where ET_c is sugarcane evapotranspiration (mm day^{-1}), and K_c is a dimensionless quantity.

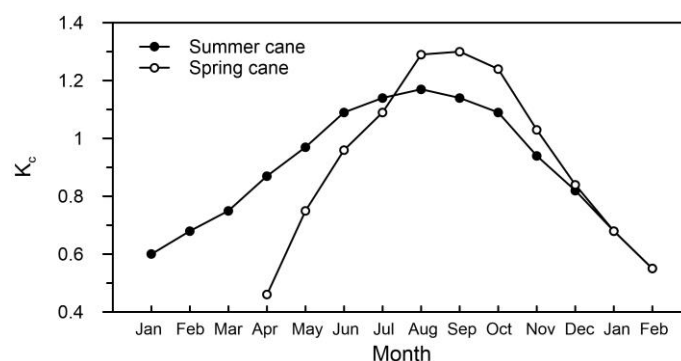


Figure 3. Annual variations in crop coefficients of summer cane and spring cane on Miyako Island (1980–2003).

2.6. Conversion from MOD16A2 and SSEBop ET to Sugarcane ET

Based on land classification, crop land accounts for 75.1% of the catchment, while the other 24.9% is bare land, roads, and residential houses. Since 24.9% of the land area has low ET, MODIS and SSEBop ET for crop land was converted by dividing 0.75 from the original ET to obtain the ET for sugarcane or ET_c for sugarcane crop evapotranspiration.

2.7. Estimation of Irrigation Water Requirement of Sugarcane

The actual irrigation water requirement from the aquifer is related to crop mixture, percentage of cropland, and irrigated area.

Since infiltration capacities were usually high in the aquifer and soil water storage change can be neglected, the difference between precipitation and actual evapotranspiration can be used to estimate recharge [58]. The monthly Crop Water Requirement (CWR) or Net Irrigation Water Requirement (NIWR) of sugarcane was calculated following the FAO method given at <https://www.fao.org/3/w4347e/w4347e0c.htm>, accessed on 15 October 2021 [59]:

$$CWR = NIWR = ET_c - P, \quad (3)$$

where P is monthly precipitation in the catchment.

According to local irrigation data, only 41% of the pumped water is delivered to the home catchment for irrigating 75% of the catchment area covered by crop land, while about 59% of the water is used in the neighboring catchments. Thus, the irrigation water requirement (hereafter irrigation requirement) from the aquifer was obtained by multiplying 0.75 (which is 100% from the catchment aquifer used to irrigate 75% of the catchment area that is cropland) and then dividing it by 0.41 to obtain actual irrigation water depth (mm) pumped from the artificial aquifer (i.e., 1.83 times NIWR when $ET_c - P$ is positive). In

other words, when 1.0 mm of irrigation water was required, 1.83 mm of water was pumped from the aquifer, as Gross Irrigation Water Requirement (GIWR). The gross irrigation water requirement is calculated as

$$GIWR = \frac{NIWR \cdot \frac{S_{crop}}{S_{catchment}}}{\alpha} = \frac{S_{crop} \cdot NIWR}{S_{catchment} \cdot \alpha} \quad (4)$$

where S_{crop} is the cropland area in the catchment; $S_{catchment}$ is the catchment area, and α is the proportion of pumped water delivered to the home catchment.

2.8. Water Table and Storage

The 2006–2021 Miyako Land Improvement District (LID) data were used to obtain monthly water table data in the catchment (Figure 1). Based on monthly groundwater table data, groundwater storage was calculated using the official H–Q formula for converting water table (m) to groundwater storage (m^3). In order to determine the correlation between groundwater storage, rainfall, and the gross irrigation water requirement, the volume of groundwater was divided by the area of the catchment and converted it into millimeters:

$$GWS_{mm} = GWS_{m^3} / S_{catchment} \quad (5)$$

where GWS_{mm} and GWS_{m^3} are groundwater storage in mm and m^3 , respectively.

2.9. Long-Term Water Storage Changes in Response to the Irrigation Requirement

Water storage change in the aquifer is explained by the following three processes: (i) water storage drop due to irrigation or GIWR ($ET_c - P > 0$); (ii) water storage rise due to precipitation or when $P - ET_c > 0$; and (iii) stabilized water storage when over-recharged rainfall spills out of the dam to the sea, or around 1.05 times the maximum groundwater storage.

Thus, GIWR ($ET_c - P > 0$) is pumped from the aquifer for irrigation as

$$GWS_{mm_t} = GWS_{mm_{t-1}} + GIWR, \quad (6)$$

where t is month t ; and $t - 1$ is early month $t - 1$.

Otherwise, when $NIWR < 0$ mm or irrigation is not required, extra precipitation replenishes the aquifer as

$$GWS_{mm_t} = GWS_{mm_{t-1}} + P - ET_c, \quad (7)$$

when GWS_{mm} is higher than 1.05 times the maximum GWS_{mm} , or when groundwater slightly overflows from the dam, water storage is stable and is expressed as:

$$GWS_{mm_t} = 1.05 \text{ times maximum } GWS_{mm} \quad (8)$$

Finally, the water storage will be no less than 0 mm.

3. Results

3.1. Reliability of Estimated Crop Evapotranspiration

In Figure 4, crop evapotranspiration obtained by the three methods (FAO-based ET_c , MOD16 model, and SSEBop model) were compared. Figure 4a shows that the monthly variations in three ET estimates were similar, while the results of both MOD16 and SSEBop were slightly lower than that of ET_c for sixteen years.

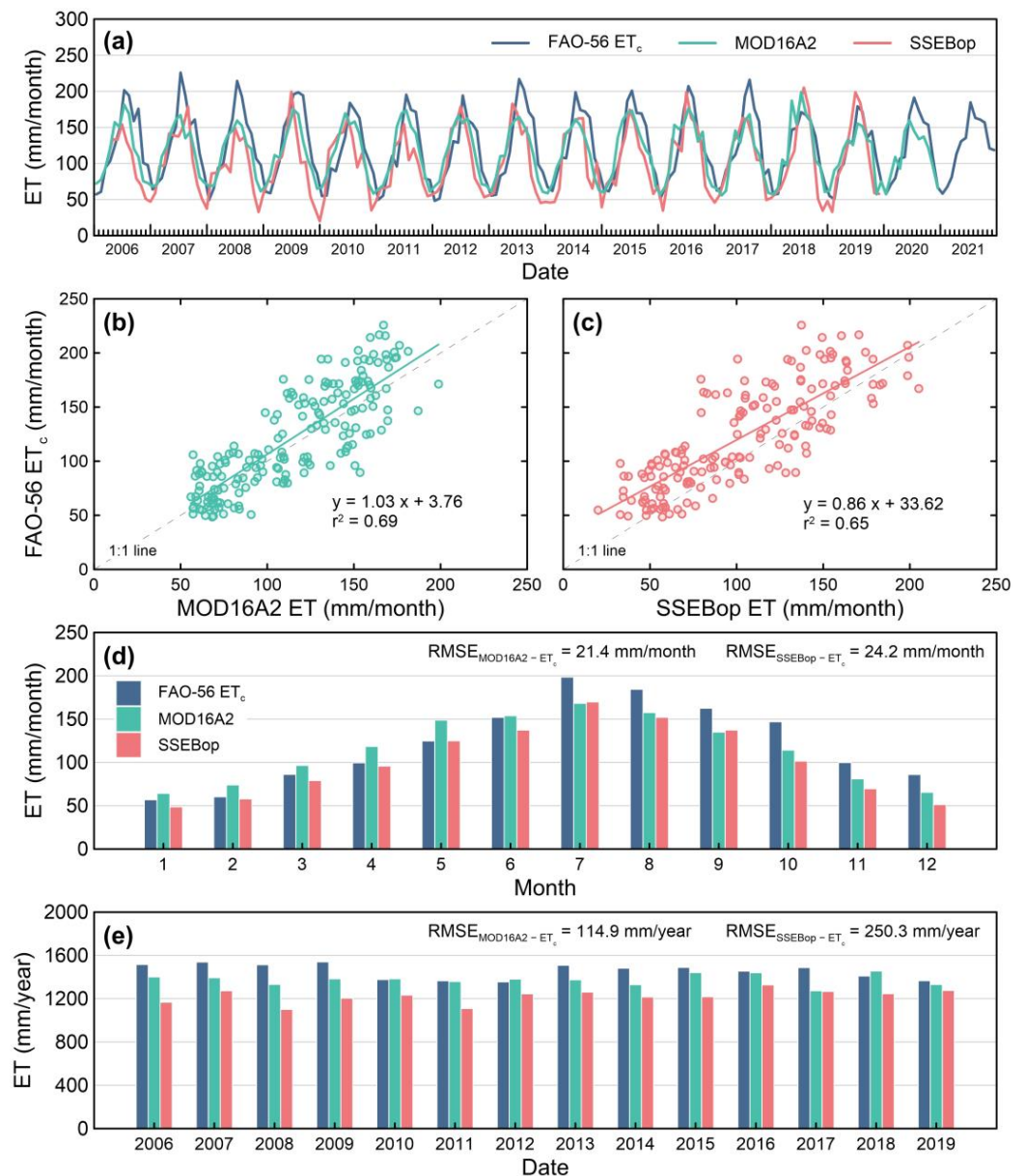


Figure 4. Comparison of three ET estimations (ET_c , MOD16A2, and SSEBop) for 2006–2019. (a) Monthly variations in comparison; (b) correlation of actual crop evapotranspiration (ET_c) and MOD16A2 ET; (c) correlation between ET_c and SSEBop ET; (d) comparison of average ET for each month; (e) comparison of annual ET from three estimates. RMSE is root mean square error.

To understand the similarity of the two ET products to the FAO56-based method, the correlation between the MOD16A2 ET and FAO-56 ET_c and that between SSEBop ET and FAO-56 ET_c are plotted in Figure 4b,c. Strong positive correlations were obtained for both the MODIS-based models, with $r^2 = 0.69$ for MOD16A2 ET and $r^2 = 0.65$ for SSEBop ET. The slope of the best-fit line for MOD16A2 ET was 1.03, which was better than that of the best-fit line for SSEBop ET. MOD16A2 ET data performed very similarly to ET_c compared to SSEBop ET in terms of both slope and r^2 .

Figure 4d shows the comparison of monthly average crop evapotranspiration for 2006–2019. Seasonally, the three estimates were very similar, with high values in summer and low values in winter. Additionally, the annual evapotranspiration values from the three estimates were compared, as seen in Figure 4e. The range of the FAO-56 ET_c was 1355.3–1539.6 mm, with an annual average of 1458.2 mm. Then the range of MOD16 ET

was 1273.1–1455.2 mm, with an annual average of 1377.0 mm, and the SSEBop ET range was 1101.3–1327.2 mm, with an annual average of 1224.6 mm. The annual averaged ET_c value looked very close to the earlier estimated value of ET_c , namely, 1469 mm, from the field-observed actual ET in 1967–1987 and in 1999–2002 in Naha, 300 km from the Miyako island, by Hossain et al. [57]. Considering the fact that remotely sensed ET products have systematic bias due to little available ground-truth calibration [60] and the possibility of underestimation of the actual ET [61], the two remotely sensed ET estimates were relatively acceptable.

3.2. Influence of Irrigation and Precipitation on Water Table and Storage

Figure 5 show the changes in the water table and the converted groundwater storage in 2006–2021, as observed in the Miyako Land Improvement District. Two long, dry periods were notable, respectively, from June 2008 to September 2009 and from June 2014 to September 2015. During the first dry period, the groundwater level dropped from 32.25 m (1105 mm) above sea level in June 2008 to 21.30 m (373 mm) in September 2009. This represented a drop of 10.95 m (732 mm) in the 15-month period, indicating that there was heavy groundwater pumping during that short period. In the second dry period, the groundwater table dropped from 30.69 m (977 mm) in June 2014 to 22.57 m (438 mm) in September 2015, denoting a drop of 8.12 m (539 mm) within 18 months. In both dry periods, the water table dropped close to 21 m, the local warning level set to start limiting groundwater pumping. The occurrence of two dry periods in 16 years suggested that there still existed the potential risk of much stronger drought for irrigation water supply, even though annual precipitation in such a period is as high as 2091.6 mm.

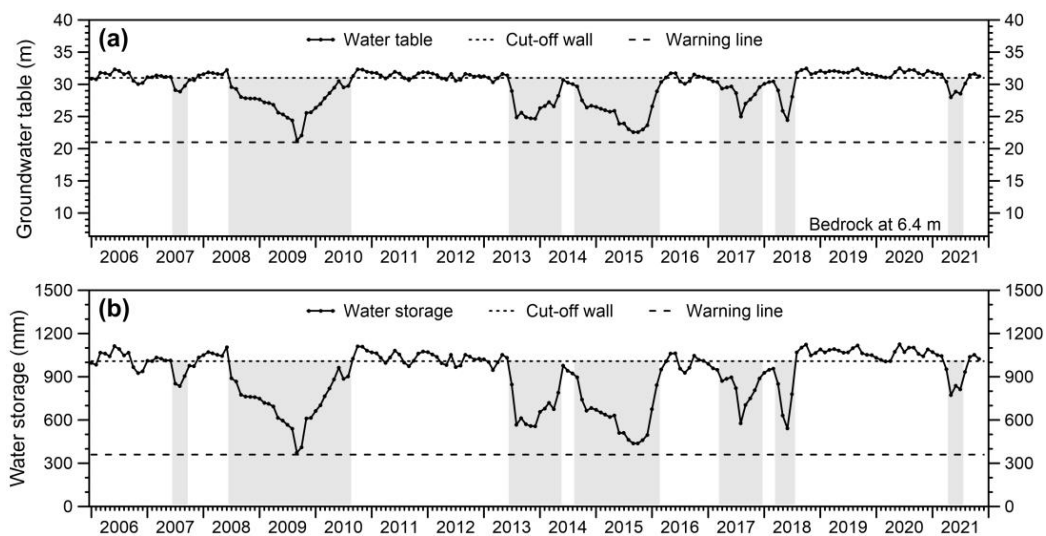


Figure 5. Changes in water table (a) and water storage (b) for the period from January 2006 to July 2021. The gray shadow in the figure indicates that the groundwater table is below 30 m.

Figure 6a shows the changes in crop evapotranspiration, corresponding with monthly precipitation since 2006. In the subtropical region, rainfall is very high but also very variable. For instance, the highest monthly precipitation in August 2018 was as high as 601.0 mm. Furthermore, the three months with the highest precipitation were August 2018, September 2017, and May 2011. On the other hand, all three ET products had a clear annual trend, driven by the generally high potential evapotranspiration and K_c in the summer period.

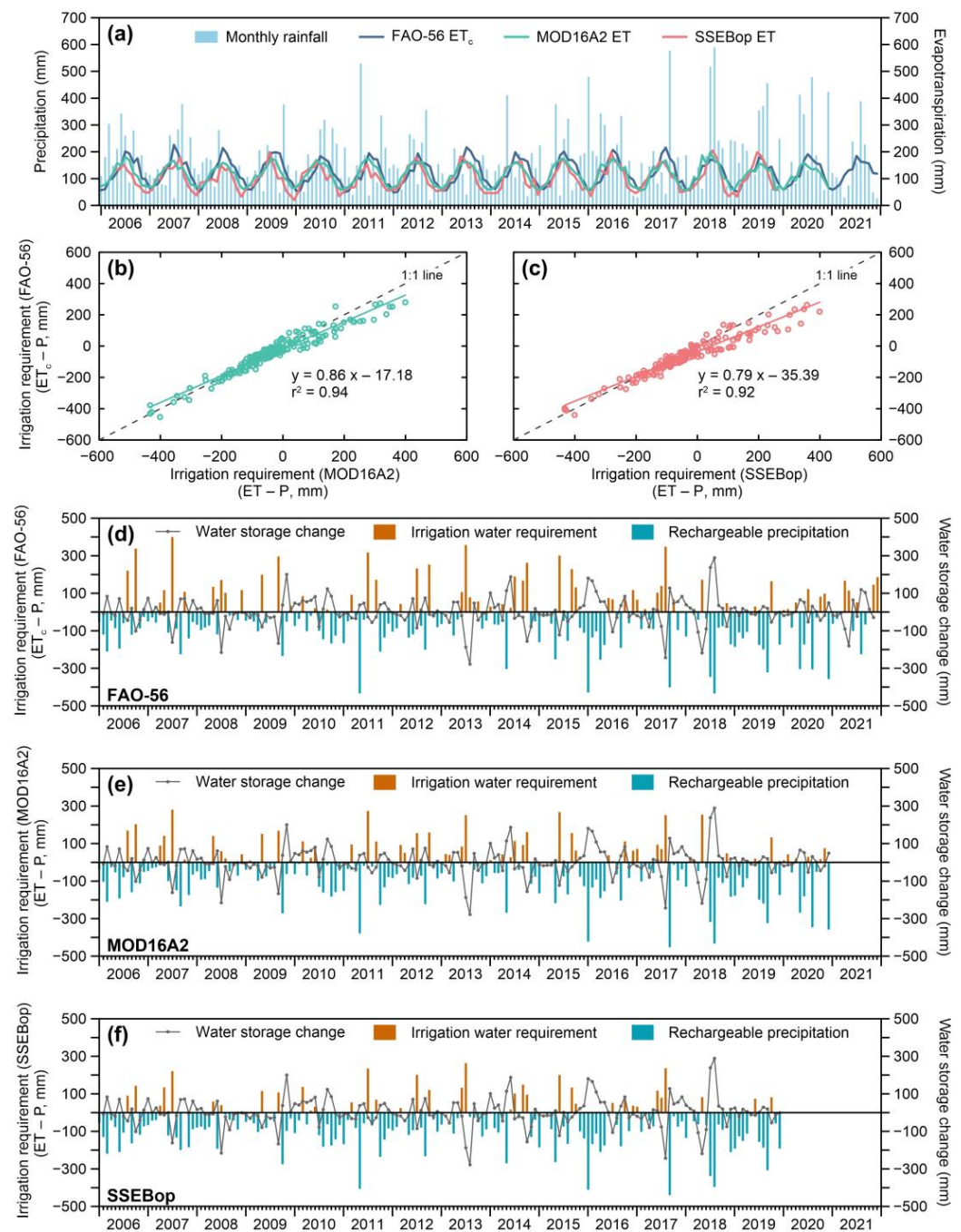


Figure 6. (a) Fluctuations in monthly rainfall and evapotranspiration (FAO-56-based ET_c, MOD16A2 ET, and SSEBop ET) for the period 2006–2021; (b) correlation between FAO-56 GIWR and MOD16A2 GIWR; (c) correlation between FAO-56 GIWR and SSEBop GIWR; (d) correspondence of water storage change to the FAO-56-based irrigation water requirement for the period 2006–2021; (e) correspondence of water storage change to the MOD16A2-based irrigation water requirement for the period 2006–2020; (f) correspondence of water storage change to the SSEBop-based irrigation water requirement for the period 2006–2019.

To understand the similarity of irrigation water requirements of the two ET products to the FAO56-based method, the correlation between the MOD16A2 GIWR and FAO-56 GIWR and that between SSEBop GIWR and FAO-56 GIWR are plotted in Figure 6b,c. Strong positive correlations were obtained for both the MODIS-based GIWR, with $r^2 = 0.94$ for MOD16A2 GIWR and $r^2 = 0.92$ for SSEBop GIWR. The slope of the best-fit line for

MOD16A2 GIWR was 0.86, which was better than that of the best-fit line for SSEBop GIWR. MOD16A2 GIWR performed very similar to the FAO-56-based GIWR than SSEBop GIWR in terms of both slope and r^2 , since SSEBop ET was lower than the other two ET products.

Figure 6d–f show the influence of each ET product on groundwater storage. Overall, the irrigation water requirement calculated from MOD16A2 and SSEBop was lower than that of FAO-56. However, the trends were very similar. Crop evapotranspiration overtook monthly precipitation in the two dry periods, resulting in the continuous monthly gross irrigation requirement ($ET - P$) depicted in Figure 6d–f. As the thin soil layer was artificially moved in and built in the catchment for crop production, soil water storage was also low, and irrigation was particularly important during times of insufficient rainfall. Based on the comparison between water storage change and the irrigation water requirement, water storage dropped whenever the monthly irrigation requirement was high. Especially in dry periods, water storage declined in most months. In contrast, when the groundwater recharge was high, water storage increased quickly.

Figure 6 shows that over the 16-year period, irrigation was necessary for a total of 62 months at an average of 3.9 months per year. This provides evidence to justify the decision to construct the artificial dam and aquifer storage area in 1993. This was especially so when the soil layer was thin and potential evaporation high in the subtropical region.

3.3. Relation between the Irrigation Water Requirement and Water Storage Changes by Three ET Methods

Figure 7 shows the relation of monthly precipitation and the gross irrigation water requirement to water storage change. Although monthly precipitation was related to water storage change ($R^2 = 0.28$ in Figure 7a), much better and significant relationships ($R^2 = 0.51$ in Figure 7b) between monthly FAO-56-based GIWR and water storage change (groundwater storage will change obviously only in the dry period, but not in the wet season since groundwater is full) illustrated the direct relevance of groundwater to crop water requirements. The comparison of r^2 values in Figure 7b–d suggested that FAO-56 GIWR may have a slightly better accuracy in estimating groundwater storage, followed by MOD16A2 and SSEBop. Furthermore, the remote sensing data are still valuable in evaluating crop irrigation water use and groundwater fluctuation.

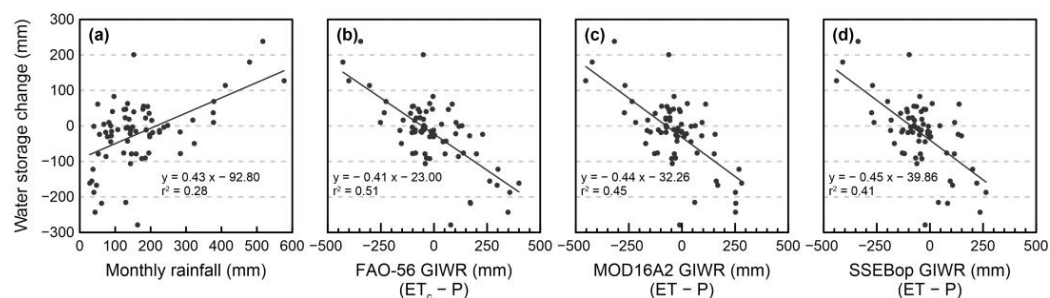


Figure 7. Correlations across precipitation, the gross irrigation water requirement, and water storage changes: correlation between water storage change and monthly rainfall (a) and correlations between monthly water storage change and GIWR (GIWR (positive value) and rechargeable rainfall (negative value) when the aquifer is not full) of FAO-56-based (b), MOD16A2 based (c), and SSEBop-based (d) values. On the y-axis, negative values refer to declines in groundwater storage, while positive values refer to groundwater recharge.

It is also suggested that there was very good agreement between the estimated gross irrigation water requirement and water storage change, especially considering the fact that irrigation water demand can change among different years along the change of crops, the expansion of the irrigation area for the neighbor catchments, and changes in farmers' irrigation practices.

3.4. Estimating Water Storage Change by Irrigation Requirements and Rechargeable Rainfall

In Figure 7b, the equation suggests that it is possible to estimate changes in groundwater storage through gross irrigation water requirement (GIWR) and precipitation recharge (ET-P). Since the MOD16A2 ET confirmed the confidence of K_c from the nearest island for the estimation of irrigation water use and precipitation recharge, the monthly water storage change from FAO-56 was compared with measured groundwater storage in 2006–2021 from the observation well in Figure 8. It shows the rough consistence between the estimated water storage and the observation. Statistical analysis suggested that the estimated value was reliable, with Nash–Sutcliffe efficiency (NSE) = 0.28, $R^2 = 0.44$, and RMSE = 102.07. The high value of RMSE = 102.07 was largely caused by the low agreement at the beginning of the estimation period from 2006 to the middle of 2008. This could be caused by the smaller irrigation area at that time, since the irrigation area is gradually expanding. It could also be due to the extensive management of irrigation by local farmers, including irregular pumping for irrigation and water storage for the next irrigation event. Additionally, the curves were similar for the lowest groundwater storage near the warning line in the two dry periods. This suggests the capability of the FAO-56 method for estimating groundwater storage using the gross irrigation water requirement and rechargeable precipitation.

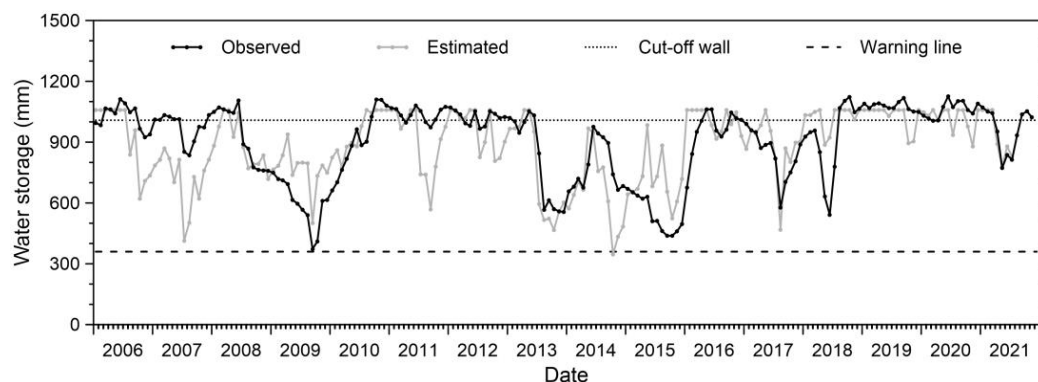


Figure 8. Comparison of estimated and observed water storage for the surface dam under the investigated period.

3.5. Crop Irrigation Requirement under Historical Climate

To further clarify the shortage of groundwater for irrigation, a much longer climate data set (1951–2021) was used to compare the difference between precipitation and crop evapotranspiration at annual and monthly scales. As seen in Figure 9a,b, annual precipitation and the estimated crop evapotranspiration (FAO-56 ET_c) were compared to clarify the long-term demand of irrigation water. Unlike Figure 4c, the relative dry years such as 2008–2009 and 2013–2014 in 2006–2021 were not really dry based on historical observation. There were five much drier years (1963, 1971, 1976, 1984, and 1993) when the annual precipitation on Miyako Island was less than the estimated FAO-56 ET_c , all of which was before the completion of the dam. Thus, there could be much more severe drought, which could cause even much more severe groundwater storage in future—much stronger than the observed dry periods such as 2008–2009 and 2014–2015 (Figure 4).

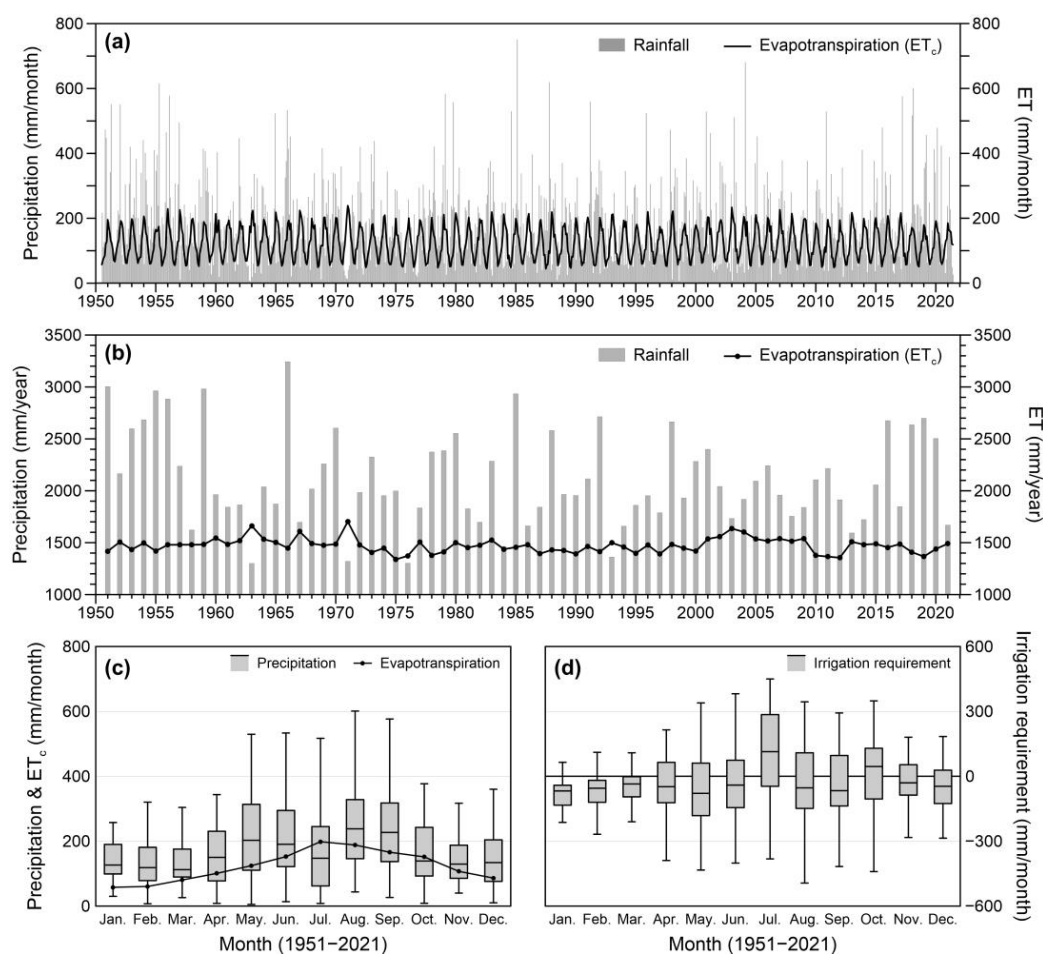


Figure 9. Comparison of precipitation and FAO-56 ET_c for the long-term: (a) corresponding monthly crop evapotranspiration and precipitation; (b) annual rainfall and crop evapotranspiration; (c) box chart of monthly precipitation and FAO-56 ET_c ; and (d) box plot of irrigation water requirement.

As seen in Figure 9b, annual water demand by sugarcane was 1339–1703 mm, while the annual rainfall on Miyako Island was 1301–3243 mm. Thus, the precipitation was sufficient to meet the amount of water required by sugarcane. However, the temporal distribution of rainfall in the island was not even, resulting in soil moisture deficiency in the summer [62]. As in Figure 9c, monthly evapotranspiration in summer sugarcane peaked in July to August. For July particularly, the average precipitation for the past few decades was only 161.7 mm, and the average monthly ET_c was 198.4 mm. In fact, ET_c was higher than precipitation in 47 out of 71 years in July. The second driest month was October, when average monthly precipitation (173.1 mm) was slightly higher than average ET_c (151.5 mm). For 36 out of 71 years, precipitation was lower than ET_c in the month of October. Then for June, August, and September, over 1/3 of the yearly precipitation was not sufficient to meet crop water requirements. For the 71 years, precipitation in 296 out of 852 months was not sufficient to meet crop water requirements. Thus, even on the subtropical island with an annual average precipitation of 2113.0 mm, irrigation was heavily and frequently needed for sugarcane production from June to October, especially in July.

3.6. Risk of Long-Term Groundwater Shortage

To understand the risk of irrigation water shortage from the aquifer under current irrigation conditions, climate data were used to estimate long-term water storage changes (Figure 10). They showed that water storage is sufficient in most of time. Furthermore, in 275 months (32% of the 852 months), water storage was full. However, in 60 months

(7% of 852 months), water storage fell below the warning line. Furthermore, in 9 months, there was completely no water for irrigation. This suggested that there was still the risk of groundwater depletion more than four times or nearly once every 18 years.

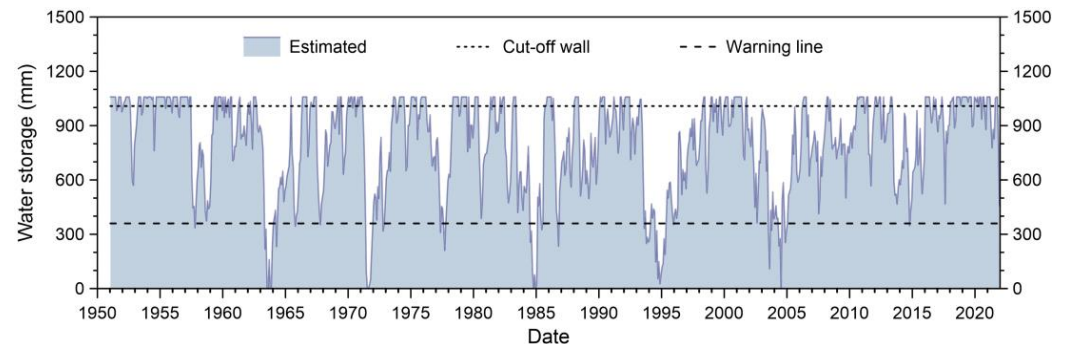


Figure 10. Estimated long-term changes in water storage under the current irrigation area and practice using 1951–2021 climate data.

3.7. Risk to Future Groundwater Shortage

To predict the risk to future groundwater storage, downscaled climate data [46] were used to assess the risk of groundwater depletion by calculating ET_c (FAO-56 based), gross irrigation water requirements, and groundwater storage changes. A time-series of groundwater storage based on four GCMs models with two emission scenarios is shown in Figure 11.

In general, similar to the results of recent studies, groundwater storage under RCP 8.5 was more prone to shortages than under RCP 2.6 [63–65]. For the RCP 2.6 scenario, groundwater storage in 88, 111, 139, and 57 out of 504 months, respectively, for GFDL-CM3, HadGEM2-ES, MIROC5, and MRI-CGCM3 models were below the local groundwater warning line in 42 years over the baseline period (1980–2021). In future climatic conditions (2022–2100), groundwater in 153, 430, 338, and 209 out of 948 months, respectively, for the four models was below the warning line. Furthermore, for the RCP 8.5 scenario, in 116, 136, 165, and 113 out of 504 months, water storage will fall below the warning line. Then, in 186, 500, 362, and 207 out of 948 months, water storage will fall below the warning line in future climatic conditions. Overall, the result suggested that the probability of groundwater shortage will increase in almost all the climate scenarios, except for the GFDL-CM3 model. This suggests that there is a higher probability of low groundwater storage under RCP 8.5 than under the RCP 2.6 scenario and a much stronger demand for dam construction in the future.

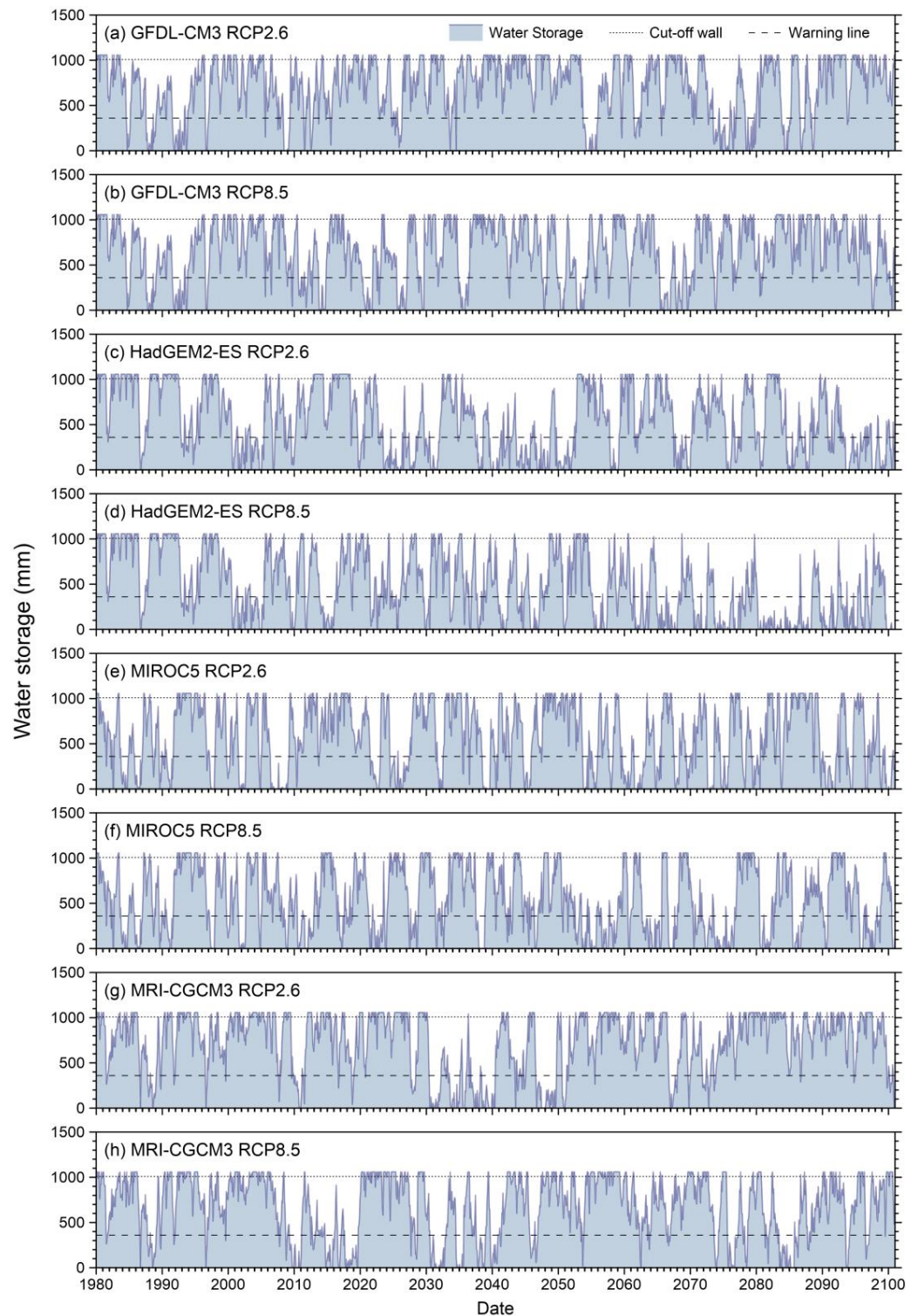


Figure 11. Time series of estimated water storage for four GCM (GFDL-CM3, HadGEM2-ES, MIROC5, and MRI-CGCM3) models under two GHG emission scenarios (RCP 2.6 and RCP 8.5) for the period 1980–2100.

4. Discussion

4.1. Effectiveness of Artificially Built Aquifer for Irrigation

In this study, the effectiveness of an artificial built aquifer in the Sunagawa Subsurface Dam on Miyako Island for irrigation was evaluated. By comparing ET_c estimated from ET_0 and K_c based on the approach of FAO-56 and MODIS-based ET products, MOD16A2

and SSEBop, it was shown that FAO-56 based ET_c and MOD16A2 are more consistent and applicable for crop evapotranspiration of sugarcane, the dominant crop on the island. It was possible to estimate the gross irrigation water requirement from the aquifer and to assess the risk of aquifer dry-up using much longer climatic data.

In the 16-year period, there were two main drought periods—one in June 2008 to September 2009 and the other in June 2014 to September 2015. In both periods, the water table nearly dropped to the local groundwater warning line set at 21 m or 35% of the effective storage of the artificial aquifer for limiting groundwater pumping [66]. Of the 192 months from January 2006 to December 2021, irrigation was required in 62 months or some 3.9 months per year. Similarly, the long-term estimate showed that in the 71 years in total, precipitation in 296 months out of 852 months or 4.2 months per year was lower than crop evapotranspiration. While crop water is mostly required in June to October, July and October were found to be the driest months. Correspondingly, irrigation water was required in 47 of the 71 years for July and 36 of the 71 years for October.

It was also shown that even in the subtropical island with annual average precipitation over 2100 mm, irrigation was heavily needed for the production of sugarcane. There could be much strong drought in the long-term that could cause total exhaustion of the aquifer. Over the 71-year assessment period, there was absolutely no water for irrigation for 9 months, suggesting the risk of groundwater dry up over four times, or nearly once every 18 years. This indicated that the current irrigation area for the neighbor catchments could not be fully covered in dry years such as 1963, 1971, 1976, 1984, 1986, 1993, and 2003. The Official Miyako Annals also recorded drought in 1963, 1971, and 2003 [67]. Therefore, with further expansion of the irrigation area, it will be difficult to guarantee the water supply from the aquifer over the dry periods.

Considering the fact that most of the soil layer in the island was artificially built and is thin (about 50 cm thick) with very limited water-holding capacity, and the fact that crop evapotranspiration from June to October can often be 6 to 8 mm daily in the subtropical climate, soil water deficit could occur soon after one rainfall or even a storm event. Thus, the construction of the dam has efficiently secured the growth of sugarcane and other crops in the catchment.

Our analysis also confirmed the important role that the artificially built aquifer has played in meeting the agricultural water supply. It can be a very valuable example for similar islands around the world.

4.2. Risks of Water Shortage under Future Climate Change

Previous studies demonstrated that climate change could lead to a more serious shortage of groundwater storage, since the impact of future climate change is likely to be negative due to the effects on irrigation water requirements [68]. For instance, Amanambu et al. [69] reviewed papers dealing with groundwater and climate change. A synthesis of 40 modeling studies suggested that future climate change will result in a decrease in groundwater storage in the humid tropics. Condon et al. [70] used a surface-groundwater hydrologic model to assess the sensitivity of shallow groundwater to climate change in the US. The result suggested that continued temperature increases could reduce groundwater storage. Salem et al. [64] discussed the impact of climate change on groundwater dynamics in irrigated regions in northwest Bangladesh using GCMs and showed significant groundwater loss with increasing temperature and near-constant rainfall. It is therefore important to evaluate the risk of groundwater shortage under future conditions [71] using climate change data to address the concerns of local residence on the periodical groundwater depletion for sugarcane production.

According to the official climate change report by the Okinawa Regional Headquarters, JMA [72], the average temperature on Miyako Island will probably increase by 3.3 °C at the end of the 21st century, and the frequency of extremely dry months will increase under the RCP 8.5 scenario. The temperature increase is expected to increase crop evapotranspira-

tion [73,74] and irrigation water demand and cause a reduction in groundwater recharge and storage.

One of the limitations of our study is the unchanged K_c value in the future climate. Without changing the K_c value, irrigation demand basically reflects the change of climate on ET_0 . However, in the real case of climate change, the K_c value could slightly change with changed phenology, especially the shortening of the seedling stage, which means an even higher crop water demand or stronger groundwater shortage in the future. However, to overcome such a limitation, we must seek the support of crop models with more experimental data, which are not available right now on the remote island.

A comparison of the estimated value for 1980–2021 in Figures 10 and 11 suggests that MRI-CGCM3 RCP 2.6 is the most acceptable model for estimating groundwater storage under the baseline period. For instance, the average groundwater storage is 724.9 mm, closest to the historical value in Figure 10 (787.5 mm). There is absolutely no water for irrigation for a period of 5 months, which is close to the historical value in Figure 10. In this model, there is a risk of groundwater dry-up for 57 months in 2022–2100, nearly 10 times higher than the historical risk. However, it is also noticeable that most of the groundwater depletion in the prediction actually occurs in a continuously dry period in 2030–2050. This could be caused by high uncertainty in the original GCMs data. Furthermore, in other GCMs models, there are also one or several drought periods in the prediction, suggesting there could be more frequent occurrences of extreme dry and wet cycles in the future [75].

Therefore, it is important to improve irrigation water management in the artificial aquifer. At the same time, as the risk of groundwater depletion both in terms of frequencies and duration under future climate will highly likely increase, new subsurface aquifer construction is needed. The study also provided valuable suggestions for water management on similar islands globally.

5. Conclusions

In this paper, on a remote island, far away from the main continent of Japan with limited experimental results on the evaluation of crop water requirements, MODIS ET together with K_c coefficient from the nearest island were compared to testify the reliability of the K_c value. Then, the testified K_c coefficient for sugarcane was used to assess the risk of irrigation water shortage using historical metrological data and to predict the future risk of irrigation agriculture under different scenarios of GCM models. The methodology developed in the study can be potentially used to evaluate long-term irrigation demand over the dry periods for engineering design or dam construction in data lacking regions globally.

Our study confirmed the important role that the artificially built aquifer played in meeting the agricultural water supply in Sunagawa Catchment and its neighbor catchments. In the 192 months from 2006 to 2021, irrigation was required in 62 months or some 3.9 months per year. Historical assessment analysis for a 71-year period from 1951 to 2021 suggested a stronger risk of groundwater dry-up, and absolutely no water for irrigation in 9 months or nearly once every 18 years. The risk of groundwater depletion both in terms of frequency and duration under future climate will highly likely increase.

The study also proved the value of ET derived from remote sensing in areas lacking the support of experimental results. It is even worthwhile to try to develop a K_c coefficient from remote sensing ET for crop irrigation assessment. However, it should be kept in mind that the percentage of high water consumptive crops in the relevant pixels should be considered to eliminate the effects of low ET components, for instance, from roads and residential areas.

Author Contributions: Conceptualization, Z.Y. and C.T.; Data curation, Z.Y.; Formal analysis, Z.Y.; Investigation, Z.Y., C.T., S.S., M.O., K.F. and G.W.; Methodology, Z.Y.; Supervision, C.T.; Writing—original draft, Z.Y.; Writing—review and editing, C.T. and H.B. All authors have read and agreed to the published version of the manuscript.

Funding: This research was funded by Research Program on Development of Innovative Technology grants from the Project of the Bio-Oriented Technology Research Advancement Institution (BRAIN) (No. 02012B).

Data Availability Statement: Metrological data is available in Japan Meteorological Agency at <http://www.data.jma.go.jp/obd/stats/etrn/index.php> (accessed on 25 October 2022). The MOD16A2 dataset can be downloaded from website: <https://lpdaac.usgs.gov/products/mod16a2v006/> (accessed on 1 December 2021). The SSEBop dataset is available in USGS FEWS NET Data Portal at <https://earlywarning.usgs.gov/fews> (accessed on 1 December 2021). The dataset on future climate change can be downloaded from website: <https://www.nies.go.jp/doi/10.17595/20200415.001-e.html> (accessed on 1 March 2022). The water table data is not publicly available.

Acknowledgments: The authors are thankful to the Miyako Land Improvement District for providing groundwater data for this research.

Conflicts of Interest: The authors declare no conflict of interest.

References

1. FAO. *Global Action Programme on Food Security and Nutrition in Small Island Developing States*; FAO: Rome, Italy, 2017; 76p.
2. Bates, B.; Kundzewicz, Z.; Wu, S. *Climate Change and Water*; Intergovernmental Panel on Climate Change Secretariat: Geneva, Switzerland, 2008.
3. Gohar, A.A.; Cashman, A.; Ward, F.A. Managing food and water security in Small Island States: New evidence from economic modelling of climate stressed groundwater resources. *J. Hydrol.* **2019**, *569*, 239–251. [[CrossRef](#)]
4. Stocker, T. *Climate Change 2013: The Physical Science Basis: Working Group I Contribution to the Fifth Assessment Report of the Intergovernmental Panel on Climate Change*; Cambridge University Press: Cambridge, UK, 2014.
5. Bailey, R.T.; Beikmann, A.; Kottermair, M.; Taboroši, D.; Jenson, J.W. Sustainability of rainwater catchment systems for small island communities. *J. Hydrol.* **2018**, *557*, 137–146. [[CrossRef](#)]
6. Campisano, A.; D’Amico, G.; Modica, C. Water Saving and Cost Analysis of Large-Scale Implementation of Domestic Rain Water Harvesting in Minor Mediterranean Islands. *Water* **2017**, *9*, 916. [[CrossRef](#)]
7. Kourtis, I.M.; Kotsifakis, K.G.; Feloni, E.G.; Baltas, E.A. Sustainable Water Resources Management in Small Greek Islands under Changing Climate. *Water* **2019**, *11*, 1694. [[CrossRef](#)]
8. Batisha, A.F. Feasibility and sustainability of fog harvesting. *Sustain. Water Qual. Ecol.* **2015**, *6*, 2. [[CrossRef](#)]
9. Tu, Y.; Wang, R.; Zhang, Y.; Wang, J. Progress and Expectation of Atmospheric Water Harvesting. *Joule* **2018**, *2*, 1452–1475. [[CrossRef](#)]
10. Elimelech, M.; Phillip, W.A. The Future of Seawater Desalination: Energy, Technology, and the Environment. *Science* **2011**, *333*, 712–717. [[CrossRef](#)] [[PubMed](#)]
11. Padrón, I.; Avila, D.; Marichal, G.N.; Rodríguez, J.A. Assessment of Hybrid Renewable Energy Systems to supplied energy to Autonomous Desalination Systems in two islands of the Canary Archipelago. *Renew. Sust. Energ. Rev.* **2019**, *101*, 221–230. [[CrossRef](#)]
12. Pistocchi, A.; Bleninger, T.; Breyer, C.; Caldera, U.; Dorati, C.; Ganora, D.; Millán, M.M.; Paton, C.; Poullis, D.; Herrero, F.S.; et al. Can seawater desalination be a win-win fix to our water cycle? *Water Res.* **2020**, *182*, 115906. [[CrossRef](#)]
13. Gu, H.; Guo, Q.; Lin, P.; Bai, L.; Yang, S.; Sitharam, T.G.; Liu, J. Feasibility Study of Coastal Reservoirs in the Zhoushan Islands, China. *J. Coast. Res.* **2019**, *2019*, 835–841. [[CrossRef](#)]
14. Holding, S.; Allen, D.M.; Foster, S.; Hsieh, A.; Larocque, I.; Klassen, J.; Van Pelt, S.C. Groundwater vulnerability on small islands. *Nat. Clim. Chang.* **2016**, *6*, 1100. [[CrossRef](#)]
15. Marston, L.; Konar, M.; Cai, X.; Troy, T.J. Virtual groundwater transfers from overexploited aquifers in the United States. *Proc. Natl. Acad. Sci. USA* **2015**, *112*, 8561–8566. [[CrossRef](#)] [[PubMed](#)]
16. Ketabchi, H.; Mahmoodzadeh, D.; Ataie-Ashtiani, B.; Werner, A.D.; Simmons, C.T. Sea-level rise impact on fresh groundwater lenses in two-layer small islands. *Hydrol. Process.* **2014**, *28*, 5938–5953. [[CrossRef](#)]
17. Underwood, M.R.; Peterson, F.L.; Voss, C.I. Groundwater lens dynamics of Atoll Islands. *Water Resour. Res.* **1992**, *28*, 2889–2902. [[CrossRef](#)]
18. Gingerich, S.B.; Voss, C.I.; Johnson, A.G. Seawater-flooding events and impact on freshwater lenses of low-lying islands: Controlling factors, basic management and mitigation. *J. Hydrol.* **2017**, *551*, 676–688. [[CrossRef](#)]
19. Bouchet, L.; Thoms, M.C.; Parsons, M. Groundwater as a social-ecological system: A framework for managing groundwater in Pacific Small Island Developing States. *Groundw. Sustain. Dev.* **2019**, *8*, 579–589. [[CrossRef](#)]
20. Ishida, S.; Tsuchihara, T.; Yoshimoto, S.; Imaizumi, M. Sustainable use of groundwater with underground dams. *Jpn. Agric. Res. Q.* **2011**, *45*, 51–61. [[CrossRef](#)]
21. McMillan, H.K.; Westerberg, I.K.; Krueger, T. Hydrological data uncertainty and its implications. *WIREs Water* **2018**, *5*, e1319. [[CrossRef](#)]

22. Fan, J.; Yue, W.; Wu, L.; Zhang, F.; Cai, H.; Wang, X.; Lu, X.; Xiang, Y. Evaluation of SVM, ELM and four tree-based ensemble models for predicting daily reference evapotranspiration using limited meteorological data in different climates of China. *Agric. For. Meteorol.* **2018**, *263*, 225–241. [[CrossRef](#)]
23. Machakaire, A.T.B.; Steyn, J.M.; Franke, A.C. Assessing evapotranspiration and crop coefficients of potato in a semi-arid climate using Eddy Covariance techniques. *Agric. Water Manag.* **2021**, *255*, 107029. [[CrossRef](#)]
24. Anapalli, S.S.; Fisher, D.K.; Reddy, K.N.; Wagle, P.; Gowda, P.H.; Sui, R. Quantifying soybean evapotranspiration using an eddy covariance approach. *Agric. Water Manag.* **2018**, *209*, 228–239. [[CrossRef](#)]
25. Yang, Y.; Anderson, M.; Gao, F.; Xue, J.; Knipper, K.; Hain, C. Improved Daily Evapotranspiration Estimation Using Remotely Sensed Data in a Data Fusion System. *Remote Sens.* **2022**, *14*, 1772. [[CrossRef](#)]
26. Anderson, M.C.; Allen, R.G.; Morse, A.; Kustas, W.P. Use of Landsat thermal imagery in monitoring evapotranspiration and managing water resources. *Remote Sens. Environ.* **2012**, *122*, 50–65. [[CrossRef](#)]
27. Elnmer, A.; Khadr, M.; Kanae, S.; Tawfik, A. Mapping daily and seasonally evapotranspiration using remote sensing techniques over the Nile delta. *Agric. Water Manag.* **2019**, *213*, 682–692. [[CrossRef](#)]
28. Allen, R.G.; Pereira, L.S.; Raes, D.; Smith, M. *Crop Evapotranspiration—Guidelines for Computing Crop Water Requirements—FAO Irrigation and Drainage Paper 56*; FAO: Rome, Italy, 1998; Volume 300, p. D05109.
29. Fisher, J.B.; Melton, F.; Middleton, E.; Hain, C.; Anderson, M.; Allen, R.; McCabe, M.F.; Hook, S.; Baldocchi, D.; Townsend, P.A.; et al. The future of evapotranspiration: Global requirements for ecosystem functioning, carbon and climate feedbacks, agricultural management, and water resources. *Water Resour. Res.* **2017**, *53*, 2618–2626. [[CrossRef](#)]
30. Liu, Y.; Qiu, G.; Zhang, H.; Yang, Y.; Zhang, Y.; Wang, Q.; Zhao, W.; Jia, L.; Ji, X.; Xiong, Y.; et al. Shifting from homogeneous to heterogeneous surfaces in estimating terrestrial evapotranspiration: Review and perspectives. *Sci. China Earth Sci.* **2022**, *65*, 197–214. [[CrossRef](#)]
31. Bawa, A.; Senay, G.B.; Kumar, S. Regional crop water use assessment using Landsat-derived evapotranspiration. *Hydrol. Process.* **2021**, *35*, e14015. [[CrossRef](#)]
32. Elnashar, A.; Wang, L.; Wu, B.; Zhu, W.; Zeng, H. Synthesis of global actual evapotranspiration from 1982 to 2019. *Earth Syst. Sci. Data* **2021**, *13*, 447–480. [[CrossRef](#)]
33. He, M.; Kimball, J.S.; Yi, Y.; Running, S.W.; Guan, K.; Moreno, A.; Wu, X.; Maneta, M. Satellite data-driven modeling of field scale evapotranspiration in croplands using the MOD16 algorithm framework. *Remote Sens. Environ.* **2019**, *230*, 111201. [[CrossRef](#)]
34. Zhang, F.; Cai, Y.; Tan, Q.; Wang, X. Spatial water footprint optimization of crop planting: A fuzzy multiobjective optimal approach based on MOD16 evapotranspiration products. *Agric. Water Manag.* **2021**, *256*, 107096. [[CrossRef](#)]
35. Sriwongsitanon, N.; Suwawong, T.; Thianpopirug, S.; Williams, J.; Jia, L.; Bastiaanssen, W. Validation of seven global remotely sensed ET products across Thailand using water balance measurements and land use classifications. *J. Hydrol. Reg. Stud.* **2020**, *30*, 100709. [[CrossRef](#)]
36. Ishida, S.; Tsuchihara, T.; Imaizumi, M. Fluctuation of NO₃-N in groundwater of the reservoir of the Sunagawa Subsurface Dam, Miyako Island, Japan. *Paddy Water Environ.* **2006**, *4*, 101–110. [[CrossRef](#)]
37. Noma, Y. Groundwater Development and Conservation in the Ryukyu Limestone Region. *J. Groundw. Hydrol.* **1992**, *34*, 163–170. [[CrossRef](#)]
38. Miyakojima City Office. *Reports on Groundwater Quality Conservation Monitoring in Miyakojima City*; Miyakojima City Office: Miyakojima, Japan, 2014.
39. Furukawa, H. Quaternary geologic history of the Ryukyu Islands. *Bull. Sci. Eng. Div. Univ. Ryukyus Math. Nat. Sci.* **1979**, *27*, 99–161.
40. Ishida, S.; Kotoku, M.; Abe, E.; Fazal, M.; Tsuchihara, T.; Imaizumi, M. Construction of subsurface dams and their impact on the environment. *RMZ Mater. Geoenviron.* **2003**, *50*, 149–152.
41. Ishida, S.; Yoshimoto, S.; Shirahata, K.; Tsuchihara, T. Distribution of NO₃-N in groundwater and groundwater flow in a reservoir area of the Sunagawa underground dam, Miyako Island, Okinawa Prefecture, Japan. *J. Groundw. Hydrol.* **2015**, *57*, 515–532. [[CrossRef](#)]
42. Nakanishi, Y. Nitrogen Outflow to Groundwater and its Control in Sub-tropic Islands. *J. Jpn. Soc. Soil Phys.* **2006**, *102*, 31–38. [[CrossRef](#)]
43. Kina, K. Actual Condition of Man-made Soils in Okinawa Prefecture. *Pedologist* **1991**, *35*, 138–144. [[CrossRef](#)]
44. Mu, Q.; Zhao, M.; Running, S.W.; Moreno, A. Improvements to a MODIS global terrestrial evapotranspiration algorithm. *Remote Sens. Environ.* **2011**, *115*, 1781–1800. [[CrossRef](#)]
45. Senay, G.B.; Bohms, S.; Singh, R.K.; Gowda, P.H.; Velpuri, N.M.; Alemu, H.; Verdin, J.P. Operational Evapotranspiration Mapping Using Remote Sensing and Weather Datasets: A New Parameterization for the SSEB Approach. *JAWRA J. Am. Water Resour. Assoc.* **2013**, *49*, 577–591. [[CrossRef](#)]
46. Ishizaki, N.N. *Bias Corrected Climate Scenarios over Japan Based on CDFDM Method Using CMIP5*; Version 202005; Center for Global Environmental Research, NIES: Tsukuba, Japan, 2020. [[CrossRef](#)]
47. Iizumi, T.; Nishimori, M.; Dairaku, K.; Adachi, S.A.; Yokozawa, M. Evaluation and intercomparison of downscaled daily precipitation indices over Japan in present-day climate: Strengths and weaknesses of dynamical and bias correction-type statistical downscaling methods. *J. Geophys. Res. Atmos.* **2011**, *116*, D01111. [[CrossRef](#)]

48. Iizumi, T.; Okada, M.; Yokozawa, M. A meteorological forcing data set for global crop modeling: Development, evaluation, and intercomparison. *J. Geophys. Res. Atmos.* **2014**, *119*, 363–384. [[CrossRef](#)]
49. Iizumi, T.; Takayabu, I.; Dairaku, K.; Kusaka, H.; Nishimori, M.; Sakurai, G.; Ishizaki, N.N.; Adachi, S.A.; Semenov, M.A. Future change of daily precipitation indices in Japan: A stochastic weather generator-based bootstrap approach to provide probabilistic climate information. *J. Geophys. Res. Atmos.* **2012**, *117*, D11114. [[CrossRef](#)]
50. Iizumi, T.; Takikawa, H.; Hirabayashi, Y.; Hanasaki, N.; Nishimori, M. Contributions of different bias-correction methods and reference meteorological forcing data sets to uncertainty in projected temperature and precipitation extremes. *J. Geophys. Res. Atmos.* **2017**, *122*, 7800–7819. [[CrossRef](#)]
51. Wiedenfeld, B.; Enciso, J. Sugarcane Responses to Irrigation and Nitrogen in Semiarid South Texas. *Agron. J.* **2008**, *100*, 665–671. [[CrossRef](#)]
52. Inman-Bamber, N.G.; McGlinchey, M.G. Crop coefficients and water-use estimates for sugarcane based on long-term Bowen ratio energy balance measurements. *Field Crops Res.* **2003**, *83*, 125–138. [[CrossRef](#)]
53. Abdul Karim, S.N.A.; Ahmed, S.A.; Nischitha, V.; Bhatt, S.; Kiran Raj, S.; Chandrashekarappa, K.N. FAO 56 Model and Remote Sensing for the Estimation of Crop-Water Requirement in Main Branch Canal of the Bhadra Command area, Karnataka State. *J. Indian Soc. Remote. Sens.* **2013**, *41*, 883–894. [[CrossRef](#)]
54. Cardoso, G.G.D.G.; Oliveira, R.C.d.; Teixeira, M.B.; Dorneles, M.S.; Domingos, R.M.O.; Megguer, C.A. Sugar cane crop coefficient by the soil water balance method. *Afr. J. Agric. Res.* **2015**, *10*, 2407–2414. [[CrossRef](#)]
55. Ferreira, E.; Mannaerts, C.M.; Dantas, A.A.; Maathuis, B.H.P. Surface energy balance system (SEBS) and satellite data for monitoring water consumption of irrigated sugarcane. *Eng. Agric.* **2016**, *36*, 1176–1186. [[CrossRef](#)]
56. Kongboon, R.; Sampattagul, S. The water footprint of sugarcane and cassava in northern Thailand. *Procedia Soc. Behav. Sci.* **2012**, *40*, 451–460. [[CrossRef](#)]
57. Hossain, M.A.; Ueno, M.; Maeda, K.; Kawamitsu, Y. Potential Evapotranspiration and Crop Coefficient Estimates for Sugarcane in Okinawa. *J. Agric. Meteorol.* **2005**, *60*, 573–576. [[CrossRef](#)]
58. Hartmann, A.; Goldscheider, N.; Wagener, T.; Lange, J.; Weiler, M. Karst water resources in a changing world: Review of hydrological modeling approaches. *Rev. Geophys.* **2014**, *52*, 218–242. [[CrossRef](#)]
59. Frenken, K. *Irrigation Potential in Africa: A Basin Approach*; Food & Agriculture Organization: Rome, Italy, 1997; Volume 4.
60. Pascolini-Campbell, M.; Reager, J.T.; Chandanpurkar, H.A.; Rodell, M. A 10 per cent increase in global land evapotranspiration from 2003 to 2019. *Nature* **2021**, *593*, 543–547. [[CrossRef](#)] [[PubMed](#)]
61. Chang, Y.; Qin, D.; Ding, Y.; Zhao, Q.; Zhang, S. A modified MOD16 algorithm to estimate evapotranspiration over alpine meadow on the Tibetan Plateau, China. *J. Hydrol.* **2018**, *561*, 16–30. [[CrossRef](#)]
62. Yamashiro, S. Studies on some elements concerned with determination of irrigation water for sugarcane in Okinawa (Department of Agricultural Engineering). *Sci. Bull. Coll. Agric. Univ. Ryukyus.* **1983**, *30*, 367–488.
63. Cochand, F.; Brunner, P.; Hunkeler, D.; Rössler, O.; Holzkämper, A. Cross-sphere modelling to evaluate impacts of climate and land management changes on groundwater resources. *Sci. Total Environ.* **2021**, *798*, 148759. [[CrossRef](#)]
64. Salem, G.S.A.; Kazama, S.; Shahid, S.; Dey, N.C. Impacts of climate change on groundwater level and irrigation cost in a groundwater dependent irrigated region. *Agric. Water Manag.* **2018**, *208*, 33–42. [[CrossRef](#)]
65. Wunsch, A.; Liesch, T.; Broda, S. Deep learning shows declining groundwater levels in Germany until 2100 due to climate change. *Nat. Commun.* **2022**, *13*, 1221. [[CrossRef](#)]
66. Imaizumi, M.; Maekawa, T.; Nagata, J.; Tomita, T. Hydrogeological simulation of Miyakojima Island subsurface dam plan. *J. Groundw. Hydrol.* **1988**, *30*, 11–23. [[CrossRef](#)]
67. Miyako Office, Okinawa Prefectural Government. *Overview of Miyako*; Miyako Office, Okinawa Prefectural Government: Miyako, Japan, 2020.
68. Taylor, R.G.; Scanlon, B.; Döll, P.; Rodell, M.; van Beek, R.; Wada, Y.; Longuevergne, L.; Leblanc, M.; Famiglietti, J.S.; Edmunds, M.; et al. Ground water and climate change. *Nat. Clim. Chang.* **2013**, *3*, 322–329. [[CrossRef](#)]
69. Amanambu, A.C.; Obarein, O.A.; Mossa, J.; Li, L.; Ayeni, S.S.; Balogun, O.; Oyebamiji, A.; Ochege, F.U. Groundwater system and climate change: Present status and future considerations. *J. Hydrol.* **2020**, *589*, 125163. [[CrossRef](#)]
70. Condon, L.E.; Atchley, A.L.; Maxwell, R.M. Evapotranspiration depletes groundwater under warming over the contiguous United States. *Nat. Commun.* **2020**, *11*, 873. [[CrossRef](#)] [[PubMed](#)]
71. Mustafa, S.M.T.; Hasan, M.M.; Saha, A.K.; Rannu, R.P.; Van Uytven, E.; Willems, P.; Huysmans, M. Multi-model approach to quantify groundwater-level prediction uncertainty using an ensemble of global climate models and multiple abstraction scenarios. *Hydrol. Earth Syst. Sci.* **2019**, *23*, 2279–2303. [[CrossRef](#)]
72. Okinawa Regional Headquarters, Japan Meteorological Agency. *Okinawa Climate Change Monitoring Report*; Okinawa Regional Headquarters, Japan Meteorological Agency: Okinawa, Japan, 2021.
73. Pour, S.H.; Wahab, A.K.A.; Shahid, S.; Ismail, Z.B. Changes in reference evapotranspiration and its driving factors in peninsular Malaysia. *Atmos. Res.* **2020**, *246*, 105096. [[CrossRef](#)]
74. Wang, Z.; Ye, A.; Wang, L.; Liu, K.; Cheng, L. Spatial and temporal characteristics of reference evapotranspiration and its climatic driving factors over China from 1979–2015. *Agric. Water Manag.* **2019**, *213*, 1096–1108. [[CrossRef](#)]
75. IPCC. *Climate Change 2021: The Physical Science Basis. Contribution of Working Group I to the Sixth Assessment Report of the Intergovernmental Panel on Climate Change*; Cambridge University Press: Cambridge, UK, 2021.